Development/Plasticity/Repair

Expressing Constitutively Active Rheb in Adult Neurons after a Complete Spinal Cord Injury Enhances Axonal Regeneration beyond a Chondroitinase-Treated Glial Scar

Di Wu,[1] Michelle C. Klaw,[1] Theresa Connors,[1] Nikolai Kholodilov,[2] Robert E. Burke,[2,3] and Veronica J. Tom[1]

[1]Department of Neurobiology and Anatomy, Drexel University College of Medicine, Philadelphia, Pennsylvania 19129, and Departments of [2]Neurology and [3]Pathology and Cell Biology, Columbia University, New York, New York 10032

After a spinal cord injury (SCI), CNS axons fail to regenerate, resulting in permanent deficits. This is due to: (1) the presence of inhibitory molecules, e.g., chondroitin sulfate proteoglycans (CSPG), in the glial scar at the lesion; and (2) the diminished growth capacity of adult neurons. We sought to determine whether expressing a constitutively active form of the GTPase Rheb (caRheb) in adult neurons after a complete SCI in rats improves intrinsic growth potential to result in axon regeneration out of a growth-supportive peripheral nerve grafted (PNG) into the SCI cavity. We also hypothesized that treating the glial scar with chondroitinase ABC (ChABC), which digests CSPG, would further allow caRheb-transduced neurons to extend axons across the distal graft interface. We found that targeting this pathway at a clinically relevant post-SCI time point improves both sprouting and regeneration of axons. CaRheb increased the number of axons, but not the number of neurons, that projected into the PNG, indicative of augmented sprouting. We also saw that caRheb enhanced sprouting far rostral to the injury. CaRheb not only increased growth rostral and into the graft, it also resulted in significantly more regrowth of axons across a ChABC-treated scar into caudal spinal cord. CaRheb $^{+}$ neurons had higher levels of growth-associated-43, suggestive of a newly identified mechanism for mTOR-mediated enhancement of regeneration. Thus, we demonstrate for the first time that simultaneously addressing intrinsic and scar-associated, extrinsic impediments to regeneration results in significant regrowth beyond an extremely challenging, complete SCI site.

Key words: **axon regeneration; chondroitinase; glial scar; Rheb; spinal cord injury; transplantation**

Significance Statement

After spinal cord injury (SCI), CNS axons fail to regenerate, resulting in permanent deficits. This is due to the diminished growth capacity of adult neurons and the presence of inhibitory molecules in the scar at the lesion. We sought to simultaneously counter both of these obstacles to achieve more robust regeneration after complete SCI. We transduced neurons postinjury to express a constitutively active Rheb to enhance their intrinsic growth potential, transplanted a growth supporting peripheral nerve graft into the lesion cavity, and enzymatically modulated the inhibitory glial scar distal to the graft. We demonstrate, for the first time, that simultaneously addressing neuron-related, intrinsic deficits in axon regrowth and extrinsic, scar-associated impediments to regeneration results in significant regeneration after SCI.

Introduction

Adult axons fail to regenerate after spinal cord injury (SCI), resulting in permanent motor, sensory, and autonomic deficits. One obstacle impeding successful regeneration of severed axons is the glial scar comprised of reactive astrocytes within the lesion penumbra, and macrophages and fibroblasts invading the lesion core (Soderblom et al., 2013; Wanner et al., 2013; Cregg et al., 2014). The scar is rich in growth inhibitory molecules, including chondroitin sulfate proteoglycans (CSPGs; Fitch and Silver, 2008; Afshari et al., 2009). Studies have shown that digesting CSPGs with the bacterial enzyme chondroitinase ABC (ChABC) improves axonal sprouting and regeneration after a SCI (Brad-

Received Feb. 22, 2015; revised July 1, 2015; accepted July 2, 2015.

Author contributions: D.W. and V.J.T. designed research; D.W., M.C.K., and T.C. performed research; N.K. and R.E.B. contributed unpublished reagents/analytic tools; D.W. and V.J.T. analyzed data; D.W. and V.J.T. wrote the paper.

This work was funded by NIH R01 NS085426 (V.J.T.), the Craig H. Neilsen Foundation nos. 280557 (D.W.) and 221439 (V.J.T.), and NIH P50 NS038370 (R.E.B.). We thank the Drexel University Spinal Cord Research Center for the use of core facilities within, and Dr Vladimir Zhukarev's assistance with the confocal microscope.

The authors declare no competing financial interests.

Correspondence should be addressed to Dr Veronica J. Tom, Department of Neurobiology and Anatomy, Drexel University College of Medicine, 2900 Queen Lane, Philadelphia, PA 19129. E-mail: veronica.tom@drexelmed.edu.

DOI:10.1523/JNEUROSCI.0719-15.2015

 0270-6474/15/3511068-13$15.00/0

bury et al., 2002; Barritt et al., 2006; Tom et al., 2009a, 2013; Starkey et al., 2012). ChABC-treatment of the scarred boundary between a growth-supportive peripheral nerve grafted (PNG) into an injury cavity and host spinal cord permits some axons to traverse the interface, synapse upon distal neurons, and mediate some functional recovery (Houle et al., 2006; Tom et al., 2009b; Alilain et al., 2011; Lee et al., 2013). Even with the removal of this inhibitor, though, only ~20% of axons emerge from the graft to reinnervate distal spinal cord. This is due to another obstacle; the diminished intrinsic capacity for growth of adult neurons.

Lower expression levels of growth-associated proteins in adulthood than in development limit a mature neuron's ability to regenerate (Blackmore et al., 2010). Mammalian target of rapamycin (mTOR) is a key regulator of protein synthesis. Decreasing levels of genes that indirectly inhibit mTOR, e.g., phosphatase and tensin homolog (PTEN), in neonatal rodents results in increased mTOR activity and axonal growth after SCI sustained in adulthood (Liu et al., 2010; Zukor et al., 2013). Although these data demonstrate the proof-of-principle that increasing the activity of protein synthesis machinery can augment axonal growth, it is important to note that in these studies, PTEN was knocked out months before the injury. Recently, Lewandowski and Steward (2014) and Danilov and Steward (2015) demonstrated that postinjury shRNA-mediated silencing of the PTEN gene in an incomplete SCI model, including in combination with injections of salmon fibrin into the lesion site to provide a growth supportive substrate, results in an increased presence of corticospinal tract fibers rostral to the injury and some caudal to injury site. It is unclear, though, how much of the effect seen was due to diminished dieback or frank regrowth. Additionally, the scar was not directly modified in either of these experiments.

Another way to activate mTOR is with a constitutively active Rheb (caRheb; Ras homolog enriched in brain), the GTPase that is directly upstream of mTOR (Durán and Hall, 2012). This version contains a point mutation that results in Rheb being persistently bound to GTP and activated (Kim et al., 2012). Here, we sought to more definitively determine whether increasing mTOR activity (via expressing caRheb) in adult neurons after complete SCI is sufficient to increase intrinsic growth capacity of mature neurons to significantly improve regeneration out of a PNG. Additionally, we hypothesized that concurrently tackling both intrinsic and extrinsic obstacles (i.e., CSPGs within the glial scar) to successful axon regeneration will be additive. To this end, we activated mTOR via caRheb postinjury and modulated the inhibitory glial scar distal to a PNG using ChABC. We found that targeting this pathway at a clinically relevant post-SCI time point improves both sprouting and regeneration of axons. Additionally, we provide data demonstrating, for the first time, that simultaneously addressing neuron-related, intrinsic deficits in axon regrowth and extrinsic, scar-associated impediments to regeneration (i.e., caRheb combined with ChABC) results in significant regeneration after SCI.

Materials and Methods

Animals. Adult female Wistar rats (225–250 g weight: Charles River Laboratories) were housed and used in accordance with Drexel University Institutional Animal Care and Use Committee and National Institutes of Health guidelines for experimentation with laboratory animals. During surgery, animals were anesthetized with isoflurane and kept on a heating pad to prevent hypothermia. After all survival surgeries, animals were given Lactated Ringer's, cefazolin (20 mg/kg), and buprenorphine (0.1 mg/kg). They were returned to their home cages once they became alert and responsive. Rats were housed two per cage with *ad libitum* access to food and water. All rats that received spinal transections had their bladders manually expressed at least twice a day for the duration of the study.

All rats receiving PNGs were given cyclosporine A (10 mg/kg, s.c., Sandimmune; Novartis Pharmaceuticals) daily starting 3 d before receiving their grafts. This immunosuppression protocol has been used previously to successfully prevent against host rejection and promote long-term survival of an intraspinal graft (Tobias et al., 2003; Houle et al., 2006).

Preparation of adeno-associated viral vectors. All single-stranded adeno-associated virus serotype 5 (AAV5) vectors were obtained from the University of North Carolina's Gene Therapy Center. The reporter green fluorescent protein (GFP) was driven by a chicken β-actin promoter. The Burke laboratory provided the plasmids to express caRheb under the control of a chicken β-actin promoter (Kim et al., 2012). This plasmid also contained a FLAG tag so that neurons transduced to express caRheb could be identified. We found that expression of the FLAG tag was restricted to the soma and was not transported down the axon (data not shown). However, GFP does fill the axoplasm following neuronal transduction (Klaw et al., 2013). Because injecting a mixture of AAVs into CNS tissue results in the vast majority of transduced neurons coexpressing both transgenes (Fan et al., 1998; Ahmed et al., 2004), we mixed AAV5-GFP with AAV5-caRheb before injection so that we could use GFP to identify the axons of caRheb-expressing neurons. We found that injecting a mixture of equivalent titers of AAV5-GFP and AAV5-caRheb-FLAG into spinal cord rostral to a spinal transection transduces the same neurons (see Fig. 6).

For caRheb-treated animals, 2 μl of AAV5-GFP (8×10^9 GC/μl) and 8 μl of AAV5-caRheb (2×10^9 GC/μl) were mixed (final titer of 1.6×10^9 GC/μl for each vector). For simplicity's sake, this will be referred to as the AAV-caRheb group. For GFP-treated animals, 2 μl of AAV5-GFP (8×10^9 GC/μl) was mixed with 8 μl of PBS for a final titer of 1.6×10^9 GC/μl.

Preparation of peripheral nerve graft. One week before grafting, tibial nerves of deeply anesthetized donor rats were isolated, ligated, and then completely severed using microscissors. The overlying musculature was sutured shut with 5-0 Vicryl and the skin was closed with wound clips. One week later, donor rats were anesthetized with ketamine (60 mg/kg) and xylazine (10 mg/kg) just before nerve harvest.

Preparation of osmotic minipumps to deliver ChABC. Osmotic minipumps (Alzet, no. 2002) were used to intrathecally deliver ChABC (Amsbio) or PBS vehicle to the graft interface for at least 2 weeks. Because ChABC alone is thermolabile, we mixed it with the sugar trehalose to thermostabilize it (Lee et al., 2010). The minipumps were prepared 1 d before implantation so that they could be primed to deliver ChABC or PBS to the injury site immediately upon placement *in vivo*. The mixture of ChABC (1U/ml) and trehalose (1 M in 0.1 M PBS) was loaded into the osmotic minipumps. An intrathecal catheter (ReCathCo) was attached to the minipump. The loaded pumps were incubated in sterile saline at 37°C overnight and were removed from the warmed saline solution just before implantation.

Transection injuries and AAV injections. A laminectomy was performed at the T6 and T7 vertebral body to expose the T7–T8 spinal cord. The dura was cut with a microknife along the rostral–caudal axis. Approximately 2 mm of spinal cord at T7 was gently removed via aspiration to completely transect (Tx) the cord. Gelfoam pledgets were placed into the cavity to achieved hemostasis. Similar to previously used methodology (Klaw et al., 2013), immediately after T7 Tx, a mixture of AAV5-caRheb and AAV5-GFP ($n = 18$; referred to as the AAV-caRheb group, for simplicity's sake) or AAV5-GFP alone ($n = 18$) was injected into spinal cord just rostral to the transection site using a glass micropipette attached to a Hamilton syringe (Fig. 1*A*). Specifically, as summarized in Figure 1*B*, 1 μl of AAV5 (1.6×10^9 GC) was slowly injected: bilaterally just medial to the lateral edge of the spinal cord at a depth of 1 and 2 mm to target the lateral and ventral funiculi; bilaterally 1 mm lateral to midline at the depth of 2.5 and 1.5 mm to target gray matter; at midline at a depth of 1 mm to target the dorsal funiculus. Thus, a total of 9 μl was injected per rat.

Just after the AAV injections were completed, four segments of predegenerated tibial nerve from a donor rat was dissected and grafted into

cavity. The PNG segments were long enough to span the lesion site (2–3 mm) and were placed such that they aligned along the dorsal–caudal axis of the spinal cord (Fig. 1*A*). The dura was stitched shut using 10-0 sutures.

The osmotic minipumps containing either ChABC ($n = 18$) or PBS ($n = 18$) were placed subcutaneously. To do this, a small incision was made in the dura above T8. The catheter was carefully threaded subdurally until the end lay just rostral to the caudal graft interface (Fig. 1*A*). The catheter was held in place via suturing to both the dura and neighboring muscle. After fixing the position of intrathecal catheter, the laminectomy site was covered with a SILASTIC membrane (BioBrane; UDL Laboratories). The overlying musculature was closed using 5-0 sutures, and the skin was closed using wound clips.

Thus, there are four groups of animals: (1) AAV-GFP + PBS ($n = 9$), (2) AAV-caRheb + PBS ($n = 9$), (3) AAV-GFP + ChABC ($n = 12$), and (4) AAV-caRheb + ChABC ($n = 12$).

True Blue labeling of neurons regenerating into PNG. A separate cohort of animals was used to identify the population of the neurons whose axons grow into the PNG via the retrograde tracer True Blue (TB; David and Aguayo, 1985; So and Aguayo, 1985; Houle, 1991; Ye and Houle, 1997; Decherchi and Gauthier, 2000). Immediately after T7 Tx, AAV-caRheb/GFP or -GFP was injected rostral to the Tx, as described above. Right after that, two segments of predegenerated tibial nerves were removed from a donor rat. For each segment, the perineurium was peeled from the proximal nerve end and the proximal end was placed into the Tx site so that it apposed the rostral wall of the lesion cavity. The nerve graft was secured by suturing perineurium to the dura using 9-0 sutures. The distal end of the PNG was covered with BioBrane and left free outside the spinal column, unapposed to any neural tissue. Dorsal muscles and the skin were closed and the rats were allowed to recover as indicated above.

One month later, graft recipient animals were anesthetized and the grafts were exposed. The distal end of the PNG was trimmed and treated with gelfoam soaked with 5% TB in distilled water to retrogradely label neurons that had grown an axon into the graft. Animals were killed and perfused transcardially with 4% PFA 1 week later. The brains and spinal cords rostral to transection were removed and 50 μm transverse sections were cut on a cryostat and collected serially. Every other section was mounted on glass slides, coverslipped using FluorSave, and examined using a Leica DM5500B microscope. All TB^+ neurons in each analyzed section was manually counted and subsequently summed for each animal. Counting was conducted while blind to the treatment group. Numbers of TB-labeled neurons in spinal cords and brainstems between animals receiving AAV-GFP or AAV-GFP/caRheb injections were compared with a Student's *t* test ($p < 0.05$; GraphPad, Prism 5).

Injecting Fluorogold into spinal cord caudal to graft. To determine the source of axons that regenerate out of the PNG, animals received a T7 Tx, injections of AAV-GFP ($n = 3$) or AAV-caRheb/GFP ($n = 3$) rostral to the transection site, grafts of PN to fill the cavity, and intrathecal delivery of thermostabilized ChABC to the distal graft interface via osmotic minipump, as described above. Three months after the T7 Tx injury and grafting, animals were anesthetized with isoflurane. The T7 Tx site was exposed and a laminectomy was performed to remove the T9 vertebral body. With a pulled glass pipette attached to a Hamilton syringe, 0.08 μl Fluorogold (FG; 1% in distilled water; Fluorochrome) was injected into nine different sites (similar to AAV injections, as described above) in the spinal cord 7 mm caudal to the PNG. FG was injected so far caudal to where we saw regrown axons to prevent diffusion of the tracer into the PNG, which would result in labeling neurons that did not extend beyond the PNG. Thus, only neurons that extended axons out of the PNG were able to take up the tracer and retrogradely transport it to their soma rostral to the Tx/PNG site.

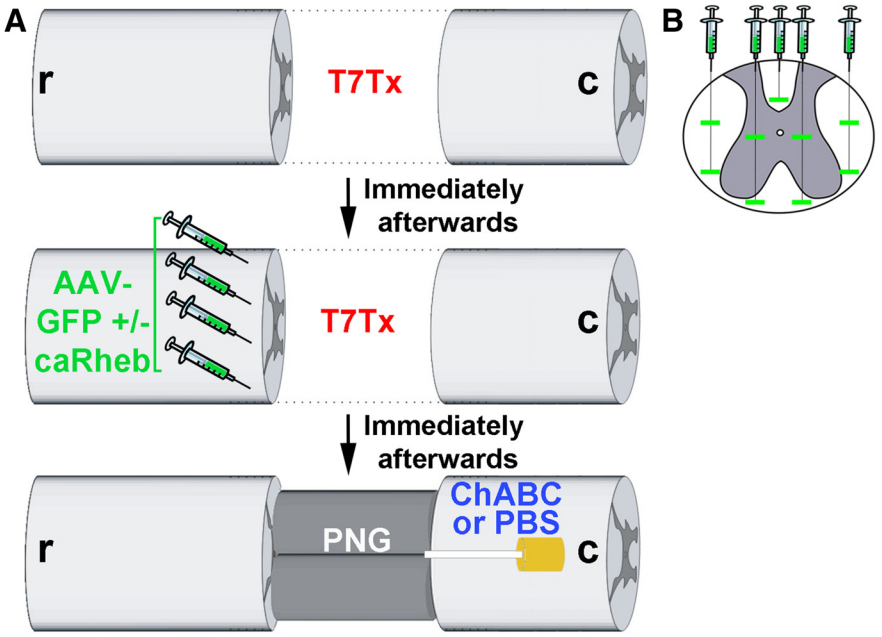

Figure 1. Schematic of the transection and grafting paradigm. ***A***, Spinal cord of adult rats was completely transected at T7. Immediately after transection, AAV5-GFP or AAV5-caRheb mixed with AAV-GFP was injected into spinal cord immediately rostral to the injury site. After the injections were completed, segments of predegenerated PN were grafted into the transection site. A catheter attached to an osmotic minipump was placed to continuously deliver ChABC or PBS vehicle to the caudal graft-host interface. ***B***, Schematic of a transverse section of spinal cord illustrates the nine locations where AAV was injected into rostral spinal cord. R, Rostral; C, caudal.

Animals were perfused 1 week later. Brains and spinal cord rostral to the Tx were sectioned and mounted on slides. All FG^+ cells were counted in sections 50 μm apart and compared using a one-way ANOVA and *post hoc* Fisher's LSD ($p < 0.05$, criterion for significance). Analysis was done blinded to the treatment group.

Histology. At 1 or 3 months after Tx and grafting ($n = 3$ per experimental group per time point), animals were killed with Euthasol and perfused with ice-cold 0.9% saline followed by ice-cold 4% PFA. The spinal cords and brains were dissected out, postfixed in the same fixative overnight at 4°C, and then cryoprotected in 30% sucrose for at least 48 h. Tissues were embedded in OCT and cut on a cryostat. Thirty micrometer horizontal sections of spinal cord tissue containing the graft and tissue 5 mm rostral and 10 mm caudal to the lesion site were cut serially. Thirty micrometer brain sections were cut transversely and collected serially. Sections were blocked in 5% normal goat serum, 10% BSA, 0.1% Triton X-100 in PBS for 1 h. After blocking, sections were incubated with anti-GFP (1:500; Millipore) to visualize axons of transduced neurons, anti-FLAG (1:1000; Sigma-Aldrich) to visualize neurons transduced to express caRheb, anti-phosphorylated ribosomal protein S6 (p-S6; 1:800; Cell Signaling Technology) to indicate mTOR activity; anti-growth-associated protein-43 (GAP-43; 1:800; Millipore); anti-glial fibrillary acidic protein (GFAP; 1:500; Millipore) to visualize astrocytes in host spinal cord, anti-postsynaptic density protein 95 (PSD-95; 1:400, Cell Signaling Technology) to visualize a postsynaptic scaffolding component of glutamatergic synapses anti-vesicular glutamate transporter 2(VGLUT2; 1:2000, Millipore) to indicate glutamatergic axons, anti-synaptophysin (1: 400; Millipore), a presynaptic component, CS-56 (1: 400; Sigma-Aldrich) to visualize intact CSPG, or anti-C-4S (1:400; Millipore) to visualize ChABC-digested CSPG "stubs." After overnight incubation with primary antibodies at 4°C, sections were washed, incubated with appropriate AlexaFluor-conjugated secondary antibodies (Invitrogen) for 2 h, washed in PBS, mounted onto slides, and coverslipped with FluorSave (EMD Chemical). Stained sections were analyzed on Olympus BX51 and Leica DM5500B epifluorescent microscopes and

a Leica TCS SP2 confocal microscope equipped with a Leica DMRE microscope.

Semithin sections. To quantify the number of axons that grew into the PNGs, a portion from the middle of the grafts from animals injected with AAV5-GFP ($n = 3$) or AAV5-GFP/caRheb ($n = 3$) was processed for plastic-embedded, semithin sectioning, as done previously (Tom et al., 2009b). Briefly, 6 months after grafting into a T7 Tx site, animals were perfused with 4% paraformaldehyde and the grafts were dissected out and postfixed overnight. The grafts were then placed into 0.1 M phosphate buffer the next day. Before embedding, the grafts were immersed in 1% osmium tetroxide, rinsed in PBS, and stained in 2% uranyl acetate. The tissue was then washed and dehydrated in a series of ascending graded alcohols from 70 to 100%. After that, the tissue was treated with propylene oxide and then incubated in a 2:1 solution of Epon/propylene oxide overnight. The following day, the tissue was changed into a mixture of Epon-812 and Araldite and then embedded into silicone molds. The molds with the grafts were placed in a 60°C oven for 3 d to polymerize the plastic. All materials were obtained from Electron Microscopy Sciences. After embedment, 1-μm-thick transverse sections of the grafts were cut on a Reichert ultramicrotome.

Myelinated axons were quantified with NIH ImageJ using well established methodology (Islamov et al., 2002; McMurray et al., 2003; Wu et al., 2012). Quantification was performed blind to treatment group. Briefly, four high-magnification (40×) bright-field images were captured using an Olympus BX51 microscope from each transverse section of the PNG. These images were then stitched together so that the entire section was visible in the montage. Myelinated axons were manually counted in five equivalently sized and similarly located regions from each individual 40× image: the upper left, upper right, lower left, lower right, and center of each image. In total, 20 regions were sampled from each PNG section to cover all portions of the graft. Importantly, each region contained axons throughout to avoid artificially decreasing axon numbers. Four transverse sections per animal were analyzed in this fashion. The average density of myelinated axons was determined and used to calculate a total number of myelinated axons per graft, based on the total size of the graft. The total numbers of axons in the PNG were compared with a Student's t test ($p < 0.05$, criterion for significance).

Quantitation of axons regenerating beyond PNG. Serial 30-μm-thick horizontal sections of the spinal cord 1 and 3 months after injury were cut on a cryostat. Regenerated axons of neurons transduced to express GFP or caRheb/GFP were visualized using immunostaining against GFP. The interface between the PNG and caudal spinal cord tissue was visualized with immunofluorescence staining against GFAP. GFP$^+$ axons beyond the GFAP$^+$ host interface were examined in a subset of sections per rat, i.e., every sixth section (180 μm intervals). Regenerating axons at different distances below the PNG/distal spinal cord tissue interface were counted using an Olympus BX51 microscope that had an ocular micrometer. The counting was conducted blind to treatment group. Axons were binned into six categories based on the distance they traveled beyond to the caudal graft edge (0–250, 251–500, 501–750, 751–1000, 1001–1500, and 1501–2000 μm). The numbers of axons per distance in each section were summed for each rat subset. The numbers of axons at each length among the four groups of animals were compared for statistical significance using a one-way ANOVA followed by a Bonferroni correction ($p < 0.05$, criterion for significance; GraphPad Prism 5).

Quantification of GAP-43 and p-S6 staining in neurons. To assess numbers of transduced supraspinal neurons expressing GAP-43 or p-S6, brainstem sections 300 μm from animals 1 month after receiving AAV-GFP or AAV-caRheb injections rostral to a Tx were processed for immunohistochemistry for GFP and GAP-43 or p-S6 as described above. All sections were processed at the same time to minimize variability.

Using immunohistochemistry methodology described above, spinal cord sections 15 mm rostral to the injury site were collected from animals 3 months after T7 Tx and injection of AAV-GFP or AAV-caRheb/GFP. Every sixth section (each 300 μm apart) from each animal was immunostained for GFP and GAP-43 or p-S6.

All images of the GFP/GAP-43 or GFP/p-S6 stained sections were acquired using equivalent exposure time settings. Using ImageJ, GFP$^+$ and GAP-43$^+$ or p-S6$^+$ neurons were counted in similarly thresholded images. The percentage of GFP$^+$ neurons that also expressed GAP-43 or p-S6 was calculated and compared among groups using a Student's t test ($p < 0.05$, criterion for significance; GraphPad Prism 5).

Results

Expressing caRheb in CNS neurons after SCI activates proteins downstream of mTOR

We first wanted to make sure that the viral vectors we were using effectively transduced neurons. Propriospinal and supraspinal neurons are capable of retrogradely transporting AAV after SCI (Klaw et al., 2013). Here, we injected AAV5-GFP or AAV5-caRheb into spinal cord tissue rostral to a T7 Tx site immediately after the transection. Four weeks later, we found that many neurons within the spinal cord and brainstem expressed GFP (Fig. 2*A*) or FLAG (tag for caRheb vector; Fig. 2*D*) in their soma, indicating that the viral vectors were effective and transduced a broad range of neurons.

One downstream target of Rheb-mediated activation of mTOR is S6 ribosomal protein (Long et al., 2005; Liu et al., 2010). To provide evidence that the caRheb was functional in our hands, we determined whether expressing caRheb in neurons after SCI increases phosphorylation (p), and thus activation, of S6. Brainstem sections from animals 1 month after injury and AAV injection were immunostained for p-S6 and GFP or FLAG to visualize transduced neurons. Although some nontransduced neurons (Fig. 2*E*, asterisk) and control, GFP$^+$ neurons expressed p-S6, many GFP$^+$ neurons did not (Figs. 2*A–C*, arrowheads). On the other hand, significantly more FLAG$^+$, caRheb$^+$ neurons (Fig. 2*D*, arrows) expressed p-S6 (~80%; Figs. 2*E*,*F*, arrows, *G*; $p < 0.05$). This pattern was observed in the spinal cord as well (Fig. 2*H*). These data suggest that expressing caRheb in CNS neurons after SCI activates the mTOR pathway.

ChABC digests CSPGs in the scar and the PNG *in vivo*

In the past, we delivered ChABC via microinjections directly into the parenchyma to digest CSPGs secreted by reactive astrocytes in the glial scar (Tom and Houlé, 2008; Tom et al., 2009b). Although ChABC delivered in this fashion is active for at least 10 d (Lin et al., 2008), we wanted to extend the length of time that bioactive ChABC would be available because it could take at least 10 d before axons injured at a thoracic level regenerate into a PNG (Amin and Houle, 2010). We postulated that delivering thermostabilized ChABC (Lee et al., 2010) intrathecally to the lesion/graft site via osmotic minipump would effectively digest scar-associated CSPGs over a prolonged period of time. To determine whether this was true, we perfused animals 3 months after T7 Tx, grafting of PN into the fresh lesion cavity, and 2 week intrathecal delivery of ChABC or PBS starting acutely after injury. Horizontal sections containing the PNG and spinal cord caudal to the graft were immunostained with antibodies against intact CSPGs (CS-56) or the four-sugar stub that remains following ChABC-digestion (C-4-S). In PBS-treated animals, the scarred boundary between the PNG and host spinal cord tissue displayed strong CS-56 staining (Figs. 3*A*,*C*), indicating that glial scar was rich in intact CSPGs. There was also a lot of staining in the PNG, indicating that the PNG is abundant in CSPGs, as found previously (Zuo et al., 1998). There was virtually no C-4-S staining in these animals (Figs. 3*B*,*C*). On the other hand, in ChABC-treated animals, we observed less intense CS-56 immunoreactivity in the PNG and almost none in the parenchyma caudal to the injury

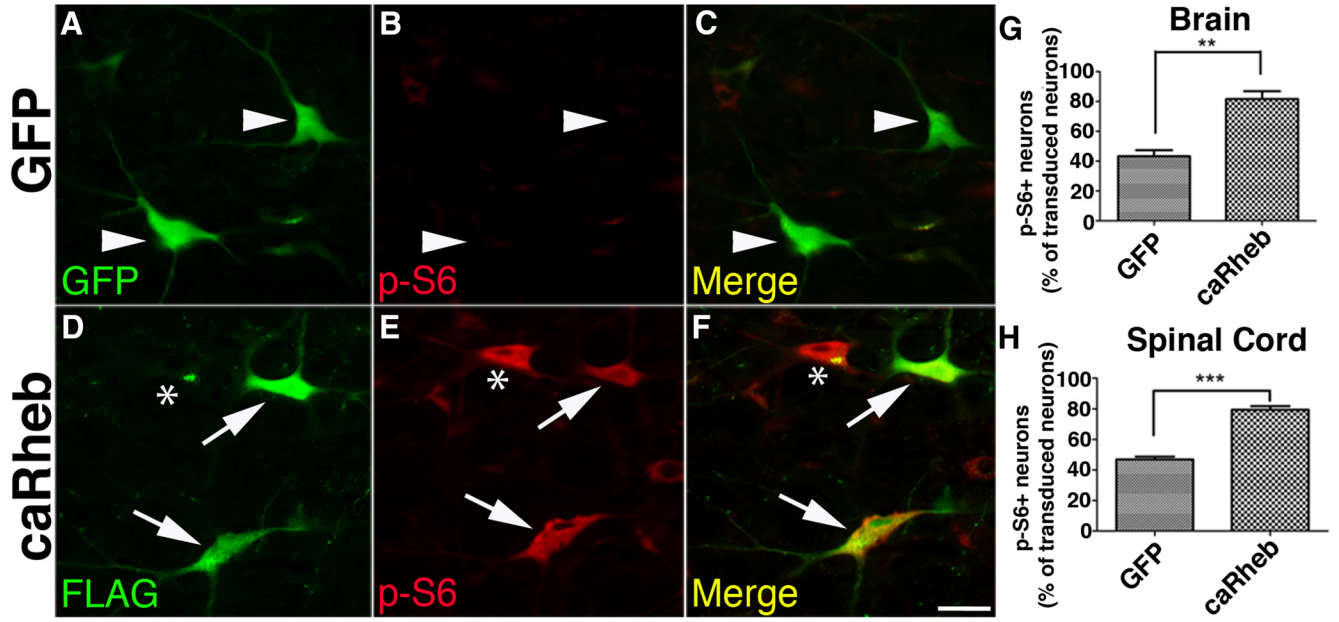

Figure 2. Transduction of neurons with AAV-caRheb induces p-S6. Brainstem sections from rats 4 weeks after receiving AAV-GFP injection or caRheb were stained for GFP and FLAG, respectively, (green) and p-S6 (red). AAV-GFP transduced neurons (***A***, arrowheads) did not show immunoreactivity for p-S6 (***B***, arrowheads). The merged image confirms that neurons expressing GFP control did not express p-S6 (***C***). Although some FLAG $^{-}$ neurons that were not transduced by AAV-caRheb (***D***, asterisk) expressed p-S6 (***E***, ***F***, asterisk), significantly more FLAG $^{+}$, AAV-caRheb transduced neurons (***D***, ***F***, arrows) had high levels of p-S6 (***E***, ***F***, arrows). ***G–H***, Quantification of the percentage of transduced neurons that were also p-S6 $^{+}$. In both brainstem (***G***) and spinal cord (***H***), the caRheb-expressing animals had a significantly higher percentage of transduced, GFP $^{+}$ or FLAG $^{+}$ neurons that were also immunoreactive for p-S6. $^{**}p < 0.01$, $^{***}p < 0.005$; $N = 3$; mean ± SEM indicated. Scale bar, 50 μm.

(Figs. 3*D*,*F*). Furthermore, there was abundant C-4-S staining in these regions (Figs. 3*E*,*F*), indicating that intrathecally delivering ChABC for at least 2 weeks was effective and resulted in long-term digestion of CSPGs within the glial scar.

caRheb expression promotes growth of axons into a PNG

Degrading CSPGs with ChABC is not necessary to attract injured axons into a PNG (Tom et al., 2009b). However, it is possible that expressing caRheb in neurons after injury will improve their ability to regenerate into a PNG. Six months after T7 Tx, virus injections, and grafting, semithin sections containing the grafts were processed to identify myelinated axons that extended into the PNG. The numbers of myelinated axons in the grafts were counted using well established methodology (Islamov et al., 2002; McMurray et al., 2003; Wu et al., 2012). As expected, there was considerable regrowth into a PNG in both the AAV-GFP and -caRheb groups. In the animals treated with just AAV-GFP, thousands of myelinated axons grew into the graft (Figs. 4*A*,*C*). Expressing caRheb in neurons after injury significantly increased that number (Figs. 4*B*,*C*; $p < 0.05$). These data indicate that caRheb expression promoted growth of axons into a PNG.

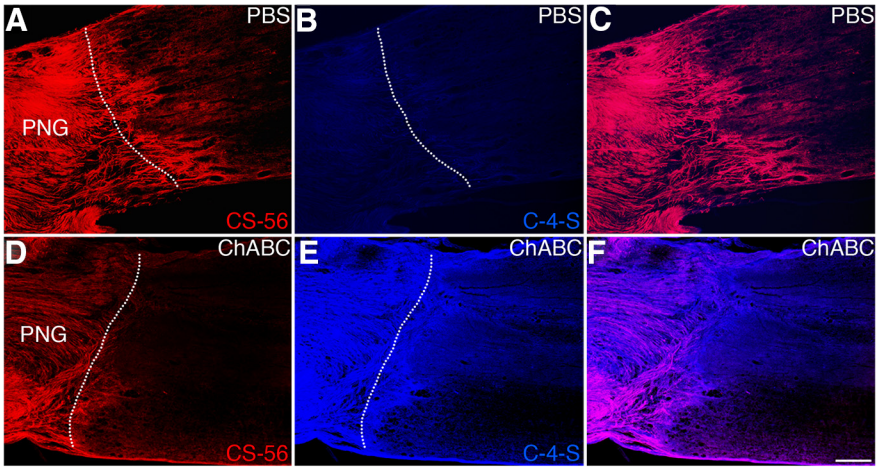

Figure 3. Continual intrathecal delivery of thermostabilized ChABC digests CSPG in the glial scar. Horizontal sections of spinal cord from animals 3 months after PBS or ChABC was intrathecally administered to the PNG/ caudal spinal cord interface via minipump for at least 2 weeks. Sections were stained with CS56 to visualize intact CSPG (red) or C-4-S, the sugar stub that remains following ChABC-digestion (blue). The merged images are shown in ***C*** and ***F***. The dashed lines indicate the boundary between PNG and caudal spinal cord tissue. After PBS treatment, there was a high level of intact CSPG in spinal cord and the PNG (***A***, ***C***) and no detectable C-4-S (***B***, ***C***). In contrast, tissue treated with ChABC exhibited high immunoreactivity for C-4-S (***E***, ***F***) and much less for CS56 (***D***, ***F***). Scale bar, 200 μm.

Propriospinal neurons project axons into the PNG

Principally propriospinal neurons and very few supraspinal neurons regenerate into a PN grafted into a lower level SCI site, such as T7 (Richardson et al., 1984). The methodology we used to inject AAV results in transduction of propriospinal neurons and multiple populations within the brainstem (Klaw et al., 2013). Thus, we wanted to determine whether expressing caRheb in supraspinal neurons improved regeneration of descending axons into a PNG. To do so, 1 month after grafting a PN into T7 Tx animals injected with AAV-GFP or -caRheb, the tracer TB was applied to the distal end of the PNG to retrogradely label neurons that regenerated axons into the graft. We primarily observed TB $^{+}$

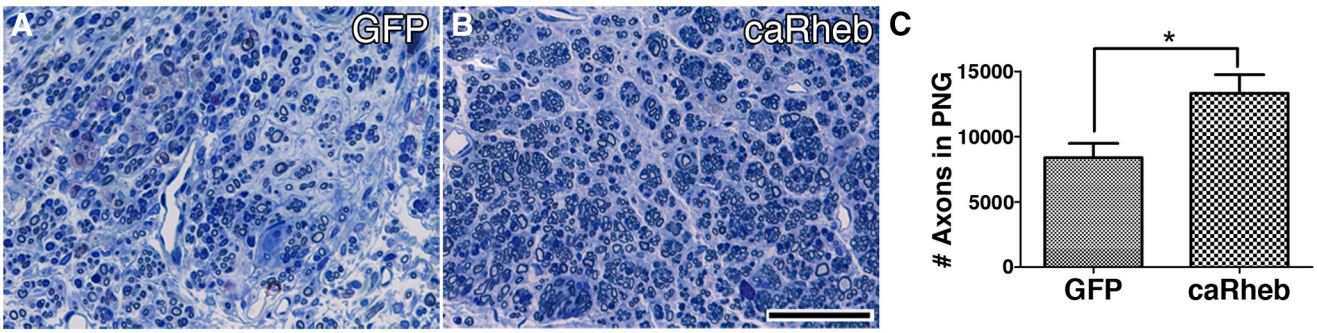

Figure 4. caRheb expression promotes axonal growth into a peripheral nerve graft. Segments of PN that were grafted into the T7 Tx sites from animals transduced with AAV-GFP (***A***) or -caRheb (***B***) were processed for semithin sectioning to assess the number of myelinated axons grew into the transplant. Though many myelinated axons were found to have extended into the PNG in both groups, the number of myelinated axons in PNG is significantly higher in the caRheb animals (***C***). Scale bar, 50 μm. Mean ± SEM indicated. $N = 3$; * = $p < 0.05$.

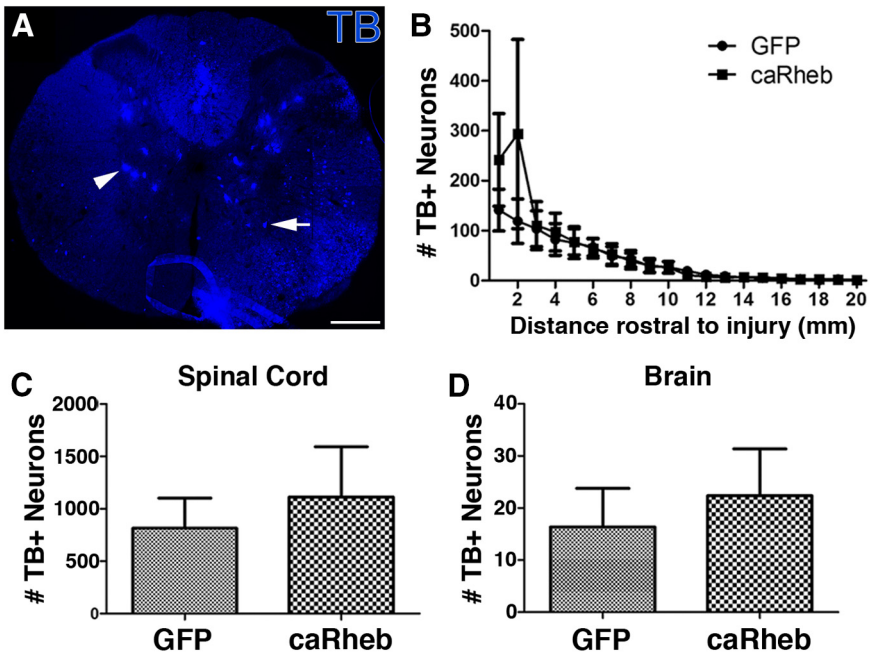

Figure 5. Axons extending into the peripheral nerve graft are mainly from propriospinal neurons. The retrograde TB tracer was placed on the exposed distal end of PNG 1 month after grafting to identify which neurons projected axons into the PNGs following transduction with either AAV-GFP or -caRheb. TB^+ neurons were counted in a subset of sections. In both groups, most TB^+ neurons were propriospinals in close proximity to injury site, as seen in the image of a representative section in ***A*** and in the graph in ***B***. A few neurons were located within the brain (***D***). There was no significant difference in the total number of TB^+ neurons between groups in either spinal cord (***C***) or in the brain (***D***). Mean ± SEM indicated. $N = 3$. Scale bar, 300 μm.

neurons distributed bilaterally in the spinal cord rostral to the injury. Most labeled neurons were close to the injury site (i.e., T5 and T6 spinal cord levels; Figs. 5*A*,*B*) and in the intermediate gray (Fig. 5*A*, arrowhead) and ventral horn (Fig. 5*A*, arrow). There was no significant difference in the number of TB^+ neurons in the cord between the two groups (Fig. 5*C*).

We found very few TB^+ neurons in the brain in both caRheb- and GFP-transduced animals (Fig. 5*D*). These neurons were located in the reticular formation and vestibular nuclei. No TB^+ neurons were observed in cortex (data not shown). Thus, current data indicate that caRheb expression does not result in more neurons projecting axons into the PNG. The neurons whose axons regenerated into the grafts originated mainly from propriospinal neurons in close proximity to the injury site.

Combining caRheb expression in neurons and ChABC treatment of the glial scar enhances axon growth beyond a PNG

We first assessed whether caRheb expression in neurons would induce more axons to emerge from the graft in the absence of glial scar modification. Though caRheb-expressing neurons contained FLAG in their somas (Fig. 2*D*), we did not detect FLAG in any axons (data not shown). Thus we sought to use GFP, which is transported down the axon and fills the axoplasm (Klaw et al., 2013), to identify axons extending from transduced neurons. We found that injecting a mixture of AAV-GFP and AAV-caRheb intraspinally transduces virtually the same neurons (Fig. 6); virtually every GFP^+ cell (Fig. 6*A*,*C*) was also $FLAG^+$ (Fig. 6*B*,*C*), indicating that we can indeed use GFP to visualize axons from neurons expressing caRheb.

When the boundary between the distal PNG and caudal spinal cord tissue was treated with PBS in animals injected with just AAV-GFP, the vast majority of GFP^+ axons in the graft remained trapped by the glial scar (Fig. 7*A*). We observed that few GFP^+ axons had extended 0–250 μm beyond the graft–host interface into spinal cord when assessed 1 (Fig. 8*A*) or 3 months later (Fig. 8*B*), similar to results from our previous studies (Houle et al., 2006; Tom et al., 2009b, 2013). Expressing caRheb did not increase the number of axons at either time point when PBS vehicle was administered to the interface (Figs. 7*B*, 8). In both conditions, even fewer axons were found at longer distances from the interface. These data indicate that expression of caRheb alone is not sufficient to enhance regeneration across an intact, inhibitory glial scar.

As we showed before, ChABC digestion of the scar at the distal graft interface significantly increased the numbers of axons that grew out of the PNG and into host tissue. In animals injected with just AAV-GFP and intrathecally administered ChABC, significantly more axons were found coursing through the $GFAP^+$ rich interface (Fig. 7*C*, arrowheads) than in animals treated with GFP+PBS or caRheb+PBS ($p < 0.05$;

Fig. 8). Interestingly, expressing caRheb further enhanced the ability of axons to extend beyond a ChABC-treated scar. Significantly more axons traversed the interface and into distal cord (Figs. 7*D*,*E*, arrows) at both time points (Fig. 8; $p < 0.05$). Not only did caRheb enhance the ability of axons to traverse the ChABC-treated scar, it also significantly increased the distance these axons regenerated back into spinal cord (Figs. 7*F–H*). There were significantly more GFP$^+$ axons at 500 μm caudal to the PNG interface 3 months after injury in the caRheb+ChABC-treated animals than in any of the other groups. In particular, caRheb+ChABC animals had ~1.8× more axons than GFP+ChABC animals at that distance (Fig. 8; $p < 0.05$). We also saw that combining caRheb with ChABC-modulation of the glial scar increased the number of axons 750 μm distal to the graft boundary ~2.4× (Fig. 8; $p < 0.05$). Last, we only observed GFP$^+$ axons 2 mm caudal to the lesion site in the caRheb+ChABC animals.

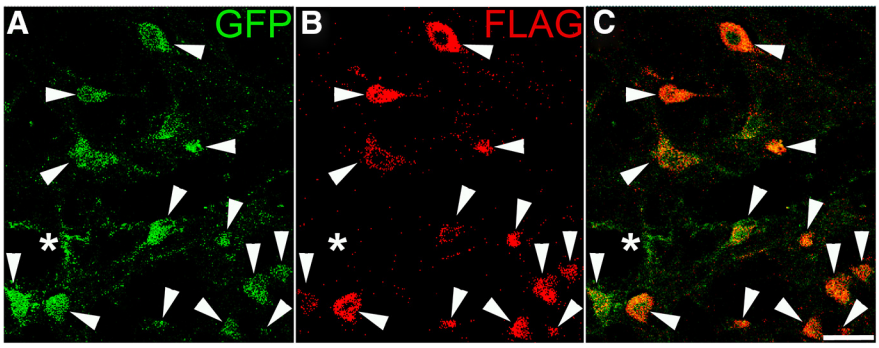

Figure 6. Injecting a mixture of AAV-GFP and -caRheb transduces the same neurons. Confocal images of a representative brainstem section 1 month after intraspinal injections of AAV-GFP and AAV-caRheb-FLAG. Virtually all GFP$^+$ (***A***, green) neurons are also FLAG$^+$ (***B***, red; arrowheads in ***A–C***), indicating that both vectors transduce the same neurons. *GFP$^+$ neuron that is FLAG$^-$, demonstrating specificity of the signal. Scale bar, 37.5 μm.

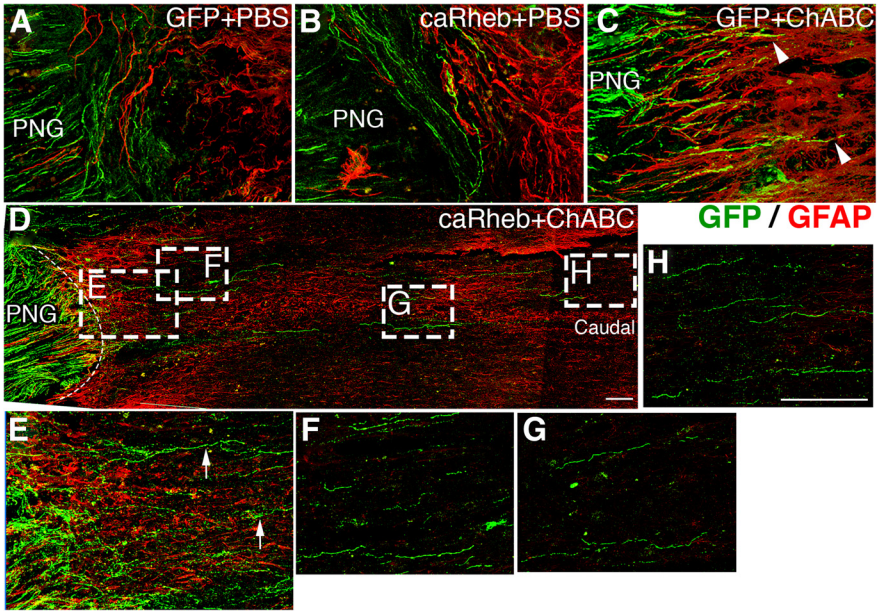

Figure 7. Expression of caRheb enhances axonal regeneration beyond a ChABC-treated PNG interface into host spinal cord tissue. Representative confocal images of horizontal sections containing the PNG and caudal spinal cord from animals 3 months after T7 Tx. Sections were immunostained for GFAP (red) to visualize astrocytes within the host spinal cord tissue and GFP (green) to identify regenerating axons. Few GFP$^+$ axons emerged from a PNG to extend into distal cord in the GFP+PBS animals (***A***) and in the caRheb+PBS animals (***B***). Modification of the scar with ChABC improved the ability of axons to traverse the interface (***C***, arrowheads). When ChABC modulation of the glial scar was combined with neuronal expression of caRheb, many more axons were able to course across the scar (***D***, ***E***, arrows) and extend for long distances within caudal spinal cord (***F–H***). Boxed regions in ***D*** are shown at higher-magnification in ***E–H***. Scale bars, 100 μm.

Axons regenerating beyond the PNG originate from propriospinal neurons

Though mainly propriospinal neurons regenerated into the PNG, some brainstem neurons did as well (Fig. 5). Thus, we sought to determine which neurons regenerated out of the PNG by injecting the retrograde tracer FluoroGold (FG) caudal to the transplant 3 months after Tx, injections of AAV-GFP or -caRheb, grafting of PN into the lesion site, and intrathecal delivery of ChABC.

As with any tracer, even a small volume of very dilute FG has the propensity to diffuse. If FG diffuses into the PNG, neurons that grew into the PNG could take the tracer up, regardless of whether or not they extended axons out of the graft. We wanted to ensure that any FG+ neurons rostral to the injury resulted from actual axonal uptake of tracer caudal to the PNG. Thus, we injected FG 7 mm caudal to the PNG, which is far from where we found regenerated axons (Fig. 8), to guarantee that FG diffused close to the PNG/spinal cord boundary but not into the PNG. Thus, only neurons that extended axons out of the PNG to where the FG diffused took up the tracer and retrogradely transported it to their cell bodies rostral to the Tx/PNG site (Fig. 9*A*,*A*′). As such, we did not observe any FG$^+$ cells rostral to the Tx in animals not treated with ChABC (Fig. 9*B*), where regeneration beyond the PNG is minimal (Fig. 8).

There were significantly more FG$^+$ neurons in rostral spinal cord in the caRheb+ChABC animals than in GFP+ChABC animals (Fig. 9C, D; $p < 0.05$). These neurons were primarily located within a few mm rostral to the injury site (Fig. 9*C*). We did not see any FG$^+$ neurons in brainstem, suggesting that the few supraspinal neurons that did regenerate into the graft did not extend axons very far, if at all, beyond the transplants, even when expressing caRheb. These data indicate that caRheb expression increases the regenerative ability of propriospinal neurons across a thoracic SCI site treated with ChABC.

Regenerating axons form putative synapses

To determine whether regenerated axons possibly formed synapses upon host neurons in spinal cord distal to the graft, sections from animals 3 months after injury and grafting were immunostained for GFP (to visualize regenerating axons) and the presynaptic marker synaptophysin. GFP$^+$ regenerating axons that penetrated the distal graft–host interface to extend into gray mat-

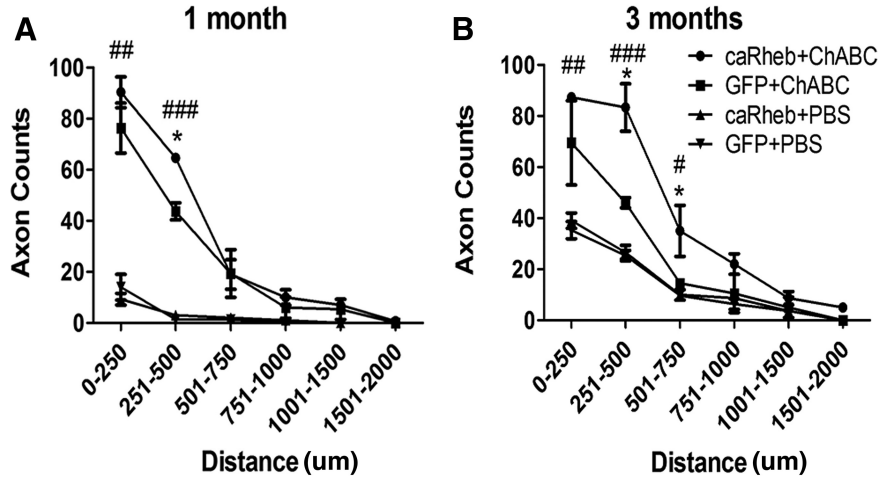

Figure 8. Quantification of axon regeneration beyond a PNG. Regenerating GFP$^+$ axons at several distances distal to the graft–host spinal cord interface were counted in a subset of sections and binned into 250 μm intervals. ***A***, One month after injury, significantly more axons grew out from the PNG 250 and 500 μm into caudal spinal cord in both ChABC-treated groups than either PBS-treated group. Additionally, there were significantly more axons 500 μm distal to the PNG in caRheb+ChABC animals than GFP+ChABC animals. ***B***, Three months after injury, significantly more axons were found 250, 500, and 750 μm caudal to the PNG in both ChABC groups than either PBS group (***B***; $^{\#}p < 0.05$, $^{\#\#}p < 0.01$, $^{\#\#\#}p < 0.005$). CaRheb+ChABC animals have significantly more axons than the other three groups 500 and 750 μm distal to the graft. Mean ± SEM indicated. $N = 3$; $^{*}p < 0.05$.

ter of host spinal cord tissue colocalized with synaptophysin (Fig. 10*A*, arrow). To provide further evidence that regenerated axons form putative synapses with appropriate synaptic machinery, we also immunostained some sections from the same animals for GFP and two critical components of functional glutamatergic synapses: PSD-95 and presynaptic VGLUT2 (Eroglu et al., 2009; Kucukdereli et al., 2011). In single-plane confocal images of these sections, we found PSD-95$^+$ puncta adjacent to VGLUT2$^+$ puncta within GFP$^+$ axons (Fig. 10*B*; arrowhead), suggestive of an excitatory, glutamatergic synapse. Collectively, these data indicate that regenerated axons formed putative synapses with appropriate presynaptic and postsynaptic machinery for a functioning synapse.

caRheb expression induces axonal sprouting in cervical spinal cord

Previous studies have reported that PTEN deletion in neonatal and young adult animals enhances compensatory axonal sprouting (Liu et al., 2010; Lee et al., 2014). Consistent with this, we observed more axons growing into the PNG after caRheb-induced mTOR activation than after AAV-GFP, despite similar numbers of neurons growing into the graft in both groups (Figs. 4, 5). To further analyze whether caRheb-expression increases axonal sprouting, we assessed GFP$^+$ axon density in gray matter of C5 spinal cord, far rostral to the T7 Tx site. The only GFP$^+$ structures visible at this level were axons; no cell bodies were labeled. In animals injected with AAV-GFP, we found some GFP$^+$ axons within the cervical intermediate gray matter (Fig. 11*A*), which is where multiple supraspinal projections normally terminate. We observed significantly more GFP$^+$ axons within intermediate gray in animals injected with AAV-caRheb (Figs. 11*B*,*C*; $p < 0.05$). These data indicate that activation of mTOR via caRheb also increases axonal sprouting rostral to a SCI site.

Increased expression of GAP-43 in neurons transduced with AAV-caRheb

Having observed enhanced axon regeneration and sprouting in the animals injected with AAV-caRheb, we wanted to begin exploring the candidate proteins that might account for such an effect. Because levels of GAP-43 have been correlated with axon growth potential (Aigner et al., 1995; Benowitz and Routtenberg, 1997; Chaisuksunt et al., 2000; Grasselli et al., 2011), we wanted to determine whether neurons transduced with caRheb have increased levels of GAP-43. One month after T7 Tx and AAV-GFP or -caRheb injection rostral to the injury site, we found many GFP$^+$ neurons in the brainstem, including in the reticular formation (Figs. 12*A*,*D*). In the AAV-GFP animals, some GFP$^+$ neurons colocalized with GAP-43 expression (Figs. 12*A*–*C*, arrow). However, most GFP$^+$ neurons did not express detectable GAP-43 (Figs. 12*A*–*C*, arrowheads). On the other hand, in the animals injected with AAV-caRheb, significantly more GFP$^+$ neurons (~1.9× more) also expressed GAP-43 (Figs. 12*D*–*F*, asterisks, *G*, $p < 0.05$). These data indicate that GAP-43 is a downstream protein target of caRheb-activated mTOR.

Discussion

As embryonic neurons mature, their intrinsic growth capacity decreases. One of the factors that limit axonal regeneration of adult neurons is the developmental regulation of proteins involved in protein synthesis, such as S6 ribosomal protein (Park et al., 2008). MTOR is part of a complex whose stimulation results in protein synthesis via phosphorylation of S6 and eukaryotic translation initiation factor 4E. Activation of the mTOR pathway has been shown to improve the intrinsic axon regenerative ability of retinal ganglion cells (Park et al., 2008), cortical neurons that project to the spinal cord via the corticospinal tract (CST; Liu et al., 2010), and DRGs (Abe et al., 2010; Christie et al., 2010; Zhou et al., 2012). These observations suggest that the level of mTOR activity is positively correlated with the growth capability of a variety of neuron types (Lu et al., 2014). However, whether stimulating the mTOR pathway promotes regeneration of all types of axons in the adult CNS remains unknown.

The means to active mTOR in this study is a mutant, constitutively active form of Rheb that exhibits resistance to GTPase inactivation (Yan et al., 2006). Rheb is active when bound to GTP and is inactive when bound to GDP. That caRheb positively affects neuronal survival and growth was previously demonstrated in a Parkinson's disease model (Kim et al., 2012). Injecting AAV-caRheb into the substantial nigra 6 weeks after a neurotoxin-induced intrastriatal lesion partially restored degenerated, nigrostriatal dopaminergic axonal projections. A very intriguing aspect of this study is that caRheb induced axonal regrowth when expressed at a postinjury time point. To our knowledge, no study has definitively established that increasing mTOR activity after a complete SCI promotes axonal regeneration of injured fibers. Here we asked whether caRheb-mediated activation of mTOR in neurons following SCI enhances axon growth. Expressing caRheb alone was not sufficient to spur regrowth of axons out of a PNG. However, combining ChABC treatment of the glial scar and neuronal caRheb expression significantly augmented the number of propriospinal axons capable of reinnervating distal spinal cord (Figs. 7, 8). Importantly, these axons formed putative

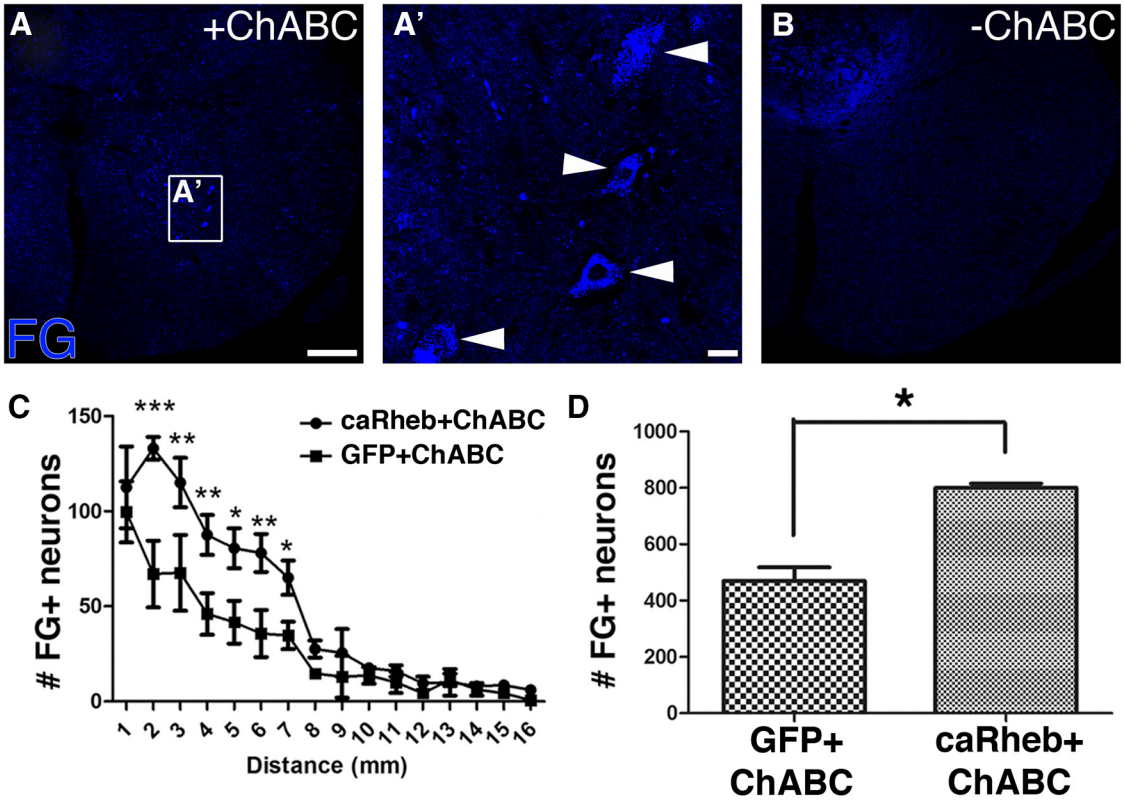

Figure 9. caRheb expression increases the number of neurons that project axons beyond a PNG. FG was injected into spinal cord 7 mm caudal to the T7 Tx and grafting site to label and identify neurons that regrew axons beyond the PNG. FG^+ neurons rostral to the Tx were only observed in animals treated with ChABC. ***A***, FG^+ neurons in a representative spinal cord section rostral to the Tx from an animal treated with ChABC. ***A'***, High-magnification image of the boxed area in ***A*** clearly indicates FG^+ neurons in rostral tissue (arrowheads). ***B***, In PBS-treated animals, where regeneration out of a PNG is minimal, FG^+ neurons were not detected in spinal cord rostral to the injury. This negative control confirms FG did not diffuse through the PNG to nonspecifically label neurons that grew into but not out of the PNG. ***C***, In both the GFP- and caRheb-transduced animals treated with ChABC, the majority of FG^+ neurons were located within 10 mm rostral to the injury. There were significantly more FG^+ neurons 2–7 mm rostral to the T7 Tx in the caRheb+ChABC animals (mean ± SEM indicated; $N = 3$; $^*p < 0.05$, $^{**}p < 0.01$). ***D***, The total number of FG^+ neurons in the caRheb+ChABC group is significantly higher than in the GFP+ChABC group ($p < 0.05$). Scale bars: ***A***, 200 μm; ***A'***, 20 μm.

synapses. The functional relevance of this regeneration will be assessed in future experiments.

MTOR is thought to enhance axon growth via increased protein synthesis, though of which proteins is not well studied. The level of growth-associated proteins, such as GAP-43 and CAP-23, is correlated with the ability of axons to extend (Kalil and Skene, 1986; Bomze et al., 2001). Interestingly, we found that caRheb resulted in more neurons expressing detectable immunoreactivity for GAP-43 (Fig. 12), elucidating a possible mechanism for the improved growth we observed. Other proteins including integrins (Condic, 2001; Andrews et al., 2009; Hawthorne et al., 2011), cytoskeletal elements like tubulin (Miller et al., 1989; Tetzlaff et al., 1991; McPhail et al., 2004), and components that transport these factors down the axon (Eva et al., 2010, 2012; Mar et al., 2014; Franssen et al., 2015) have also been implicated in regulating growth. It would be interesting to determine whether levels of these proteins are similarly altered in neurons expressing caRheb.

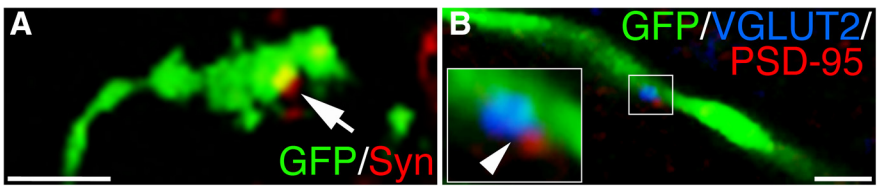

Figure 10. Regenerating axons form putative synapses. Single-plane confocal images of sections containing spinal cord distal to the PNG from animals 3 months after T7 Tx and grafting. ***A***, The presynaptic protein synaptophysin (red, arrow) is present in GFP^+ axons (green) that regenerated into host caudal spinal cord. ***B***, A GFP^+ axon (green) distal to the graft contains the glutamatergic presynaptic marker VGLUT2 (blue) that is adjacent to the postsynaptic scaffolding protein PSD-95 (red, arrowhead), suggestive of a functioning excitatory synapse. Scale bars, 5 μm.

Which neurons regenerate into a PNG is highly dependent upon the distance of the axotomy from the soma; the greater the distance, the less likely a neuron will upregulate regeneration associated genes and re-extend a severed axon (Fernandes et al., 1999; Siebert et al., 2010). Thus, a PN grafted into a thoracic SCI is virtually absent of descending axons and primarily contains axons from propriospinal neurons (Richardson et al., 1984). Expressing caRheb did not alter the total number of neurons that regenerated into the graft (Fig. 5). On the other hand, it did significantly increase the number of myelinated axons present in the PNG sections (Fig. 4), indicative of intensified sprouting. While we have evidence that caRheb resulted in more sprouting rostral to the PNG (Fig. 11), we did not analyze sequential sections of the PNG to compare the number of axons at the rostral and caudal ends of the PNG. Thus, we do not know with certainty whether the greater numbers of axons within the PNG is due to sprouting before entry into the PNG or sprouting within the PNG. Nev-

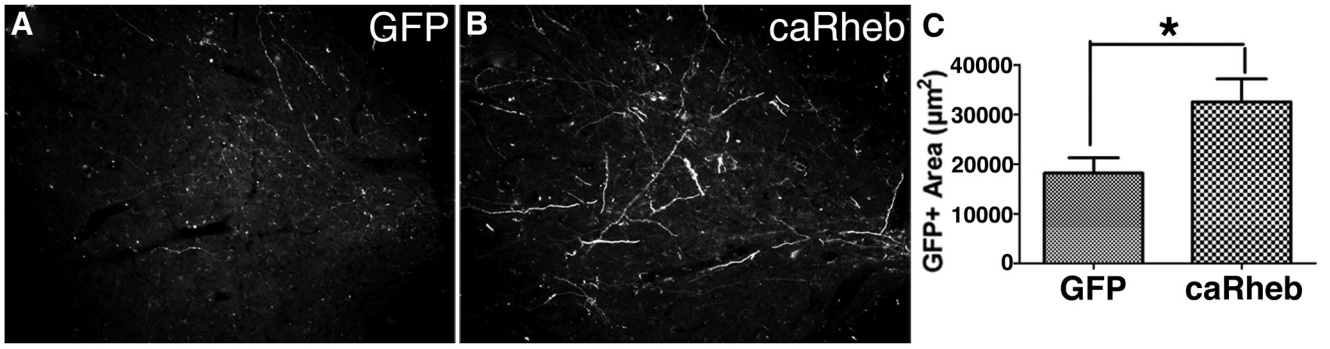

Figure 11. caRheb expression enhances axonal sprouting rostral to a SCI site. Transverse sections of C5 spinal cord were collected from animals 3 months after T7 Tx and AAV-GFP or AAV-caRheb injection. Although some GFP $^{+}$ axons are seen in AAV-GFP injected animals (***A***), significantly more GFP $^{+}$ axons are seen in AAV-caRheb transduced animals (***B***). ***C***, GFP $^{+}$ areas in thresholded images of intermediate gray were quantified for each group. Significantly more GFP was measured, indicating that caRheb promotes sprouting of axons far rostral to an injury site. $*p < 0.05$, $N = 3$. Mean ± SEM indicated.

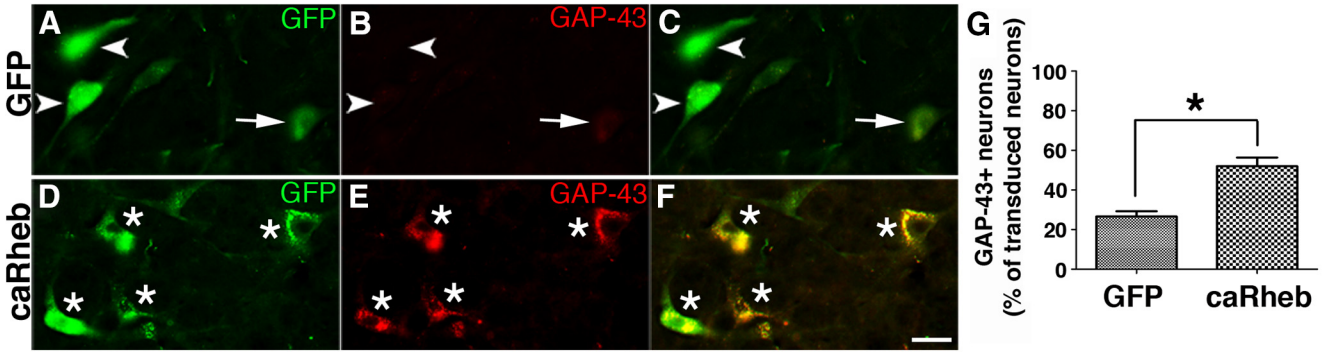

Figure 12. Transduction of neurons with AAV-caRheb induces GAP-43. Representative images of brainstem sections from AAV-GFP or -caRheb animals stained for GFP to identify transduced neurons (green) and the growth-associated protein GAP-43 (red). Though a few neurons transduced with AAV-GFP (***A***, ***C***, arrow) expressed some detectable GAP-43 (***B***, ***C***, arrow), most did not (***A***–***C***, arrowheads). On the other hand, more neurons transduced with AAV-caRheb (***D***, ***F***, asterisks) strongly expressed GAP-43 (***E***, ***F***, asterisks). ***G***, Quantification of the ratio of GFP $^{+}$ neurons that also expressed GAP-43. Expressing caRheb significantly increased the percentage of transduced, GFP $^{+}$ neurons that were immunoreactive for GAP-43 as well. $N = 3$, $*p < 0.05$. Mean ± SEM indicated. Scale bar, 50 μm.

ertheless, collectively, these data suggest that mTOR activation postinjury enhances the ability to sprout collaterals but does not necessarily enhance the ability of an adult neuron to regenerate into an extremely growth-supportive substrate such as a PNG. Because propriospinal neurons are primarily the ones that extend into the PNG here (Fig. 5), it is likely that the increased fibers we observed within the graft are of intraspinal origin. It will be important in future studies to determine whether certain populations are more susceptible to caRheb/mTOR-enhanced sprouting.

These data confirm other published data indicating that mTOR can mediate axonal branching (Grider et al., 2009; Lee et al., 2014). PTEN deletion in sensorimotor cortex of young adult rats before a unilateral pyramidotomy resulted in more sprouting of spared CST fibers into denervated, contralateral spinal cord (Lee et al., 2014). Additionally, conditionally knocking out PTEN in sensorimotor cortical neurons in young adult mice immediately after a bilateral cervical contusion injury increased arborization of CST fibers rostral to the injury (Danilov and Steward, 2015). Similarly, in the caRheb animals in this study, in which various supraspinal populations other than cortical neurons were transduced, we saw more GFP $^{+}$ axons in cervical spinal cord far rostral to the thoracic Tx site (Fig. 11).

Interestingly, increased levels of GAP-43, which is what we observed in the neurons expressing caRheb, have also been associated with increased axonal branching (Schreyer and Skene, 1993; Aigner and Caroni, 1995; Aigner et al., 1995; Buffo et al., 1997; Allegra Mascaro et al., 2013). Identifying a treatment that can be enacted after an injury that promotes significant sprouting can be an important component of a strategy to promote functional recovery after SCI. Spontaneous collateralization of a variety of populations, e.g., propriospinal and reticulospinal neurons (Bareyre et al., 2004; Ballermann and Fouad, 2006; Courtine et al., 2008; Filli et al., 2014), after incomplete SCI has been associated with behavioral recovery. Elucidating a means to further enhance this plasticity could be beneficial. Although we do not definitively know which neurons sprouted in cervical spinal cord, neurons within the reticular formation and vestibular nucleus are transduced in our model (Klaw et al., 2013). Furthermore, we have evidence that caRheb increases GAP-43 expression levels in these supraspinal populations (Fig. 12). Future experiments will expand upon this.

It has recently come to light that ChABC treatment after SCI can modulate the immune response and shift the phenotype of infiltrating macrophages from classically activated, proinflammatory M1 to alternatively activated, anti-inflammatory M2 macrophages (Bartus et al., 2014; Didangelos et al., 2014). Although invasion of M1 macrophages into spinal cord tissue after SCI are associated with cell death and lesion expansion (Blight, 1994; Popovich et al., 1999; Faulkner et al., 2004; Kroner et al., 2014), M2 macrophages are associated with repair and spurring axon growth (Kigerl et al., 2009; Busch et al., 2011). It will be interesting to determine if/how caRheb expression in neurons

after SCI affects the growth-promoting effect of ChABC-stimulated M2 macrophages.

The finding that activating mTOR in adult neurons alone does not effectively promote regeneration is not wholly surprising. These injured axons continue to express receptors, such as PTPσ (Shen et al., 2009) and LAR (Fisher et al., 2011), for growth-inhibitory CSPGs that are still intact within an unmodified scar. Moreover, when Lewandowski and Steward (2014) used AAV-shPTEN to drive mTOR activity in rat sensorimotor cortical neurons, they did not observe enhanced CST sprouting or regrowth across a lesion site. It was only when they combined PTEN knockdown with salmon fibrin did they see more CST fibers closer to the injury site, indicative of increased regrowth or diminished retraction. Other factors, e.g., SOCS3 (Sun et al., 2011), STAT3 (Bareyre et al., 2011; Lang et al., 2013), sox11 (Wang et al., 2015), c-myc (Belin et al., 2015), Krüppel-like factor-4 (KLF-4; Moore et al., 2009; Qin et al., 2013), and KLF-7 (Blackmore et al., 2012) also seem to modulate regenerative potential. Along these lines, in this study, we found that not all neurons that were transduced to express caRheb expressed GAP-43. Thus, to mount a truly robust regenerative response, it is likely that multiple proteins will need to be manipulated. Indeed, codeletion of PTEN and SOCS3 results in more retinal ganglion cell regeneration after optic nerve injury than when either is knocked down alone (Sun et al., 2011).

In conclusion, expressing caRheb to activate mTOR in neurons after SCI enhances axonal sprouting and regeneration. The latter was only seen when caRheb was combined with modulation of extrinsic, scar-associated inhibitory factors. This is the first clear demonstration that modulating mTOR in adult CNS neurons postinjury stimulates robust axonal regrowth after a complete lower level SCI, an extremely challenging injury model in which to promote regeneration of endogenous axons. In future studies, it will be important to focus on optimizing the conditions for more efficient regeneration, as well as how to shape appropriate synapse formation.

References

Abe N, Borson SH, Gambello MJ, Wang F, Cavalli V (2010) Mammalian target of rapamycin (mTOR) activation increases axonal growth capacity of injured peripheral nerves. J Biol Chem 285:28034–28043. CrossRef Medline

Afshari FT, Kappagantula S, Fawcett JW (2009) Extrinsic and intrinsic factors controlling axonal regeneration after spinal cord injury. Expert Rev Mol Med 11:e37. CrossRef Medline

Ahmed BY, Chakravarthy S, Eggers R, Hermens WT, Zhang JY, Niclou SP, Levelt C, Sablitzky F, Anderson PN, Lieberman AR, Verhaagen J (2004) Efficient delivery of Cre-recombinase to neurons in vivo and stable transduction of neurons using adeno-associated and lentiviral vectors. BMC Neurosci 5:4. CrossRef Medline

Aigner L, Caroni P (1995) Absence of persistent spreading, branching, and adhesion in GAP-43-depleted growth cones. J Cell Biol 128:647–660. CrossRef Medline

Aigner L, Arber S, Kapfhammer JP, Laux T, Schneider C, Botteri F, Brenner HR, Caroni P (1995) Overexpression of the neural growth-associated protein GAP-43 induces nerve sprouting in the adult nervous system of transgenic mice. Cell 83:269–278. CrossRef Medline

Alilain WJ, Horn KP, Hu H, Dick TE, Silver J (2011) Functional regeneration of respiratory pathways after spinal cord injury. Nature 475:196–200. CrossRef Medline

Allegra Mascaro AL, Cesare P, Sacconi L, Grasselli G, Mandolesi G, Maco B, Knott GW, Huang L, De Paola V, Strata P, Pavone FS (2013) *In vivo* single branch axotomy induces GAP-43-dependent sprouting and synaptic remodeling in cerebellar cortex. Proc Natl Acad Sci U S A 110:10824–10829. CrossRef Medline

Amin AA, Houle JD (2010) The role of neurotrophic factors and their receptors in ascending and descending axon regeneration through intraspinal peripheral nerve grafts (PNGs). In: Program #5888 2010 Neuroscience Meeting Planner, San Diego, Society for Neuroscience, 2010.

Andrews MR, Czvitkovich S, Dassie E, Vogelaar CF, Faissner A, Blits B, Gage FH, ffrench-Constant C, Fawcett JW (2009) Alpha9 integrin promotes neurite outgrowth on tenascin-C and enhances sensory axon regeneration. J Neurosci 29:5546–5557. CrossRef Medline

Ballermann M, Fouad K (2006) Spontaneous locomotor recovery in spinal cord injured rats is accompanied by anatomical plasticity of reticulospinal fibers. Eur J Neurosci 23:1988–1996. CrossRef Medline

Bareyre FM, Kerschensteiner M, Raineteau O, Mettenleiter TC, Weinmann O, Schwab ME (2004) The injured spinal cord spontaneously forms a new intraspinal circuit in adult rats. Nat Neurosci 7:269–277. CrossRef Medline

Bareyre FM, Garzorz N, Lang C, Misgeld T, Büning H, Kerschensteiner M (2011) In vivo imaging reveals a phase-specific role of STAT3 during central and peripheral nervous system axon regeneration. Proc Natl Acad Sci U S A 108:6282–6287. CrossRef Medline

Barritt AW, Davies M, Marchand F, Hartley R, Grist J, Yip P, McMahon SB, Bradbury EJ (2006) Chondroitinase ABC promotes sprouting of intact and injured spinal systems after spinal cord injury. J Neurosci 26:10856–10867. CrossRef Medline

Bartus K, James ND, Didangelos A, Bosch KD, Verhaagen J, Yáñez-Munoz RJ, Rogers JH, Schneider BL, Muir EM, Bradbury EJ (2014) Large-scale chondroitin sulfate proteoglycan digestion with chondroitinase gene therapy leads to reduced pathology and modulates macrophage phenotype following spinal cord contusion injury. J Neurosci 34:4822–4836. CrossRef Medline

Belin S, Nawabi H, Wang C, Tang S, Latremoliere A, Warren P, Schorle H, Uncu C, Woolf CJ, He Z, Steen JA (2015) Injury-induced decline of intrinsic regenerative ability revealed by quantitative proteomics. Neuron 86:1000–1014. CrossRef Medline

Benowitz LI, Routtenberg A (1997) GAP-43: an intrinsic determinant of neuronal development and plasticity. Trends Neurosci 20:84–91. CrossRef Medline

Blackmore MG, Moore DL, Smith RP, Goldberg JL, Bixby JL, Lemmon VP (2010) High content screening of cortical neurons identifies novel regulators of axon growth. Mol Cell Neurosci 44:43–54. CrossRef Medline

Blackmore MG, Wang Z, Lerch JK, Motti D, Zhang YP, Shields CB, Lee JK, Goldberg JL, Lemmon VP, Bixby JL (2012) Kruppel-like Factor 7 engineered for transcriptional activation promotes axon regeneration in the adult corticospinal tract. Proc Natl Acad Sci U S A 109:7517–7522. CrossRef Medline

Blight AR (1994) Effects of silica on the outcome from experimental spinal cord injury: implication of macrophages in secondary tissue damage. Neuroscience 60:263–273. CrossRef Medline

Bomze HM, Bulsara KR, Iskandar BJ, Caroni P, Skene JH (2001) Spinal axon regeneration evoked by replacing two growth cone proteins in adult neurons. Nat Neurosci 4:38–43. CrossRef Medline

Bradbury EJ, Moon LD, Popat RJ, King VR, Bennett GS, Patel PN, Fawcett JW, McMahon SB (2002) Chondroitinase ABC promotes functional recovery after spinal cord injury. Nature 416:636–640. CrossRef Medline

Buffo A, Holtmaat AJ, Savio T, Verbeek JS, Oberdick J, Oestreicher AB, Gispen WH, Verhaagen J, Rossi F, Strata P (1997) Targeted overexpression of the neurite growth-associated protein B-50/GAP-43 in cerebellar Purkinje cells induces sprouting after axotomy but not axon regeneration into growth-permissive transplants. J Neurosci 17:8778–8791. Medline

Busch SA, Hamilton JA, Horn KP, Cuascut FX, Cutrone R, Lehman N, Deans RJ, Ting AE, Mays RW, Silver J (2011) Multipotent adult progenitor cells prevent macrophage-mediated axonal dieback and promote regrowth after spinal cord injury. J Neurosci 31:944–953. CrossRef Medline

Chaisuksunt V, Zhang Y, Anderson PN, Campbell G, Vaudano E, Schachner M, Lieberman AR (2000) Axonal regeneration from CNS neurons in the cerebellum and brainstem of adult rats: correlation with the patterns of expression and distribution of messenger RNAs for L1, CHL1, c-jun and growth-associated protein-43. Neuroscience 100:87–108. CrossRef Medline

Christie KJ, Webber CA, Martinez JA, Singh B, Zochodne DW (2010) PTEN inhibition to facilitate intrinsic regenerative outgrowth of adult peripheral axons. J Neurosci 30:9306–9315. CrossRef Medline

Condic ML (2001) Adult neuronal regeneration induced by transgenic integrin expression. J Neurosci 21:4782–4788. Medline

Courtine G, Song B, Roy RR, Zhong H, Herrmann JE, Ao Y, Qi J, Edgerton

VR, Sofroniew MV (2008) Recovery of supraspinal control of stepping via indirect propriospinal relay connections after spinal cord injury. Nat Med 14:69–74. CrossRef Medline

Cregg JM, DePaul MA, Filous AR, Lang BT, Tran A, Silver J (2014) Functional regeneration beyond the glial scar. Exp Neurol 253:197–207. CrossRef Medline

Danilov CA, Steward O (2015) Conditional genetic deletion of PTEN after a spinal cord injury enhances regenerative growth of CST axons and motor function recovery in mice. Exp Neurol 266:147–160. CrossRef Medline

David S, Aguayo AJ (1985) Axonal regeneration after crush injury of rat central nervous system fibres innervating peripheral nerve grafts. J Neurocytol 14:1–12. CrossRef Medline

Decherchi P, Gauthier P (2000) Regrowth of acute and chronic injured spinal pathways within supra-lesional post-traumatic nerve grafts. Neuroscience 101:197–210. CrossRef Medline

Didangelos A, Iberl M, Vinsland E, Bartus K, Bradbury EJ (2014) Regulation of IL-10 by chondroitinase ABC promotes a distinct immune response following spinal cord injury. J Neurosci 34:16424–16432. CrossRef Medline

Durán RV, Hall MN (2012) Regulation of TOR by small GTPases. EMBO Rep 13:121–128. CrossRef Medline

Eroglu C, Allen NJ, Susman MW, O'Rourke NA, Park CY, Ozkan E, Chakraborty C, Mulinyawe SB, Annis DS, Huberman AD, Green EM, Lawler J, Dolmetsch R, Garcia KC, Smith SJ, Luo ZD, Rosenthal A, Mosher DF, Barres BA (2009) Gabapentin receptor $\alpha 2\delta$-1 is a neuronal thrombospondin receptor responsible for excitatory CNS synaptogenesis. Cell 139:380–392. CrossRef Medline

Eva R, Dassie E, Caswell PT, Dick G, ffrench-Constant C, Norman JC, Fawcett JW (2010) Rab11 and its effector Rab coupling protein contribute to the trafficking of beta 1 integrins during axon growth in adult dorsal root ganglion neurons and PC12 cells. J Neurosci 30:11654–11669. CrossRef Medline

Eva R, Crisp S, Marland JR, Norman JC, Kanamarlapudi V, ffrench-Constant C, Fawcett JW (2012) ARF6 directs axon transport and traffic of integrins and regulates axon growth in adult DRG neurons. J Neurosci 32:10352–10364. CrossRef Medline

Fan DS, Ogawa M, Fujimoto KI, Ikeguchi K, Ogasawara Y, Urabe M, Nishizawa M, Nakano I, Yoshida M, Nagatsu I, Ichinose H, Nagatsu T, Kurtzman GJ, Ozawa K (1998) Behavioral recovery in 6-hydroxydopamine-lesioned rats by cotransduction of striatum with tyrosine hydroxylase and aromatic L-amino acid decarboxylase genes using two separate adeno-associated virus vectors. Hum Gene Ther 9:2527–2535. CrossRef Medline

Faulkner JR, Herrmann JE, Woo MJ, Tansey KE, Doan NB, Sofroniew MV (2004) Reactive astrocytes protect tissue and preserve function after spinal cord injury. J Neurosci 24:2143–2155. CrossRef Medline

Fernandes KJ, Fan DP, Tsui BJ, Cassar SL, Tetzlaff W (1999) Influence of the axotomy to cell body distance in rat rubrospinal and spinal motoneurons: differential regulation of GAP-43, tubulins, and neurofilament-M. J Comp Neurol 414:495–510. CrossRef Medline

Filli L, Engmann AK, Zörner B, Weinmann O, Moraitis T, Gullo M, Kasper H, Schneider R, Schwab ME (2014) Bridging the gap: a reticulo-propriospinal detour bypassing an incomplete spinal cord injury. J Neurosci 34:13399–13410. CrossRef Medline

Fisher D, Xing B, Dill J, Li H, Hoang HH, Zhao Z, Yang XL, Bachoo R, Cannon S, Longo FM, Sheng M, Silver J, Li S (2011) Leukocyte common antigen-related phosphatase is a functional receptor for chondroitin sulfate proteoglycan axon growth inhibitors. J Neurosci 31:14051–14066. CrossRef Medline

Fitch MT, Silver J (2008) CNS injury, glial scars, and inflammation: inhibitory extracellular matrices and regeneration failure. Exp Neurol 209:294–301. CrossRef Medline

Franssen EH, Zhao RR, Koseki H, Kanamarlapudi V, Hoogenraad CC, Eva R, Fawcett JW (2015) Exclusion of integrins from CNS axons is regulated by Arf6 activation and the AIS. J Neurosci 35:8359–8375. CrossRef Medline

Grasselli G, Mandolesi G, Strata P, Cesare P (2011) Impaired sprouting and axonal atrophy in cerebellar climbing fibres following in vivo silencing of the growth-associated protein GAP-43. PLoS One 6:e20791. CrossRef Medline

Grider MH, Park D, Spencer DM, Shine HD (2009) Lipid raft-targetedAkt promotes axonal branching and growth cone expansion via mTOR and Rac1, respectively. J Neurosci Res 87:3033–3042. CrossRef Medline

Hawthorne AL, Hu H, Kundu B, Steinmetz MP, Wylie CJ, Deneris ES, Silver J (2011) The unusual response of serotonergic neurons after CNS injury: lack of axonal dieback and enhanced sprouting within the inhibitory environment of the glial scar. J Neurosci 31:5605–5616. CrossRef Medline

Houle JD (1991) Demonstration of the potential for chronically injured neurons to regenerate axons into intraspinal peripheral nerve grafts. Exp Neurol 113:1–9. CrossRef Medline

Houle JD, Tom VJ, Mayes D, Wagoner G, Phillips N, Silver J (2006) Combining an autologous peripheral nervous system "bridge" and matrix modification by chondroitinase allows robust, functional regeneration beyond a hemisection lesion of the adult rat spinal cord. J Neurosci 26:7405–7415. CrossRef Medline

Islamov RR, Hendricks WA, Jones RJ, Lyall GJ, Spanier NS, Murashov AK (2002) 17β-Estradiol stimulates regeneration of sciatic nerve in female mice. Brain Res 943:283–286. CrossRef Medline

Kalil K, Skene JH (1986) Elevated synthesis of an axonally transported protein correlates with axon outgrowth in normal and injured pyramidal tracts. J Neurosci 6:2563–2570. Medline

Kigerl KA, Gensel JC, Ankeny DP, Alexander JK, Donnelly DJ, Popovich PG (2009) Identification of two distinct macrophage subsets with divergent effects causing either neurotoxicity or regeneration in the injured mouse spinal cord. J Neurosci 29:13435–13444. CrossRef Medline

Kim SR, Kareva T, Yarygina O, Kholodilov N, Burke RE (2012) AAV transduction of dopamine neurons with constitutively active Rheb protects from neurodegeneration and mediates axon regrowth. Mol Ther 20:275–286. CrossRef Medline

Klaw MC, Xu C, Tom VJ (2013) Intraspinal AAV injections immediately rostral to a thoracic spinal cord injury site efficiently transduces neurons in spinal cord and brain. Mol Ther Nucleic Acids 2:e108. CrossRef Medline

Kroner A, Greenhalgh AD, Zarruk JG, Passos Dos Santos R, Gaestel M, David S (2014) TNF and increased intracellular iron alter macrophage polarization to a detrimental M1 phenotype in the injured spinal cord. Neuron 83:1098–1116. CrossRef Medline

Kucukdereli H, Allen NJ, Lee AT, Feng A, Ozlu MI, Conatser LM, Chakraborty C, Workman G, Weaver M, Sage EH, Barres BA, Eroglu C (2011) Control of excitatory CNS synaptogenesis by astrocyte-secreted proteins Hevin and SPARC. Proc Natl Acad Sci U S A 108:E440-449. CrossRef Medline

Lang C, Bradley PM, Jacobi A, Kerschensteiner M, Bareyre FM (2013) STAT3 promotes corticospinal remodelling and functional recovery after spinal cord injury. EMBO Rep 14:931–937. CrossRef Medline

Lee DH, Luo X, Yungher BJ, Bray E, Lee JK, Park KK (2014) Mammalian target of rapamycin's distinct roles and effectiveness in promoting compensatory axonal sprouting in the injured CNS. J Neurosci 34:15347–15355. CrossRef Medline

Lee H, McKeon RJ, Bellamkonda RV (2010) Sustained delivery of thermostabilized chABC enhances axonal sprouting and functional recovery after spinal cord injury. Proc Natl Acad Sci U S A 107:3340–3345. CrossRef Medline

Lee YS, Lin CY, Jiang HH, DePaul M, Lin VW, Silver J (2013) Nerve regeneration restores supraspinal control of bladder function after complete spinal cord injury. J Neurosci 33:10591–10606. CrossRef Medline

Lewandowski G, Steward O (2014) AAVshRNA-mediated suppression of PTEN in adult rats in combination with salmon fibrin administration enables regenerative growth of corticospinal axons and enhances recovery of voluntary motor function after cervical spinal cord injury. J Neurosci 34:9951–9962. CrossRef Medline

Lin R, Kwok JC, Crespo D, Fawcett JW (2008) Chondroitinase ABC has a long-lasting effect on chondroitin sulphate glycosaminoglycan content in the injured rat brain. J Neurochem 104:400–408. CrossRef Medline

Liu K, Lu Y, Lee JK, Samara R, Willenberg R, Sears-Kraxberger I, Tedeschi A, Park KK, Jin D, Cai B, Xu B, Connolly L, Steward O, Zheng B, He Z (2010) PTEN deletion enhances the regenerative ability of adult corticospinal neurons. Nat Neurosci 13:1075–1081. CrossRef Medline

Long X, Lin Y, Ortiz-Vega S, Yonezawa K, Avruch J (2005) Rheb binds and regulates the mTOR kinase. Curr Biol 15:702–713. CrossRef Medline

Lu Y, Belin S, He Z (2014) Signaling regulations of neuronal regenerative ability. Curr Opin Neurobiol 27:135–142. CrossRef Medline

Mar FM, Simões AR, Leite S, Morgado MM, Santos TE, Rodrigo IS, Teixeira CA, Misgeld T, Sousa MM (2014) CNS axons globally increase axonal

transport after peripheral conditioning. J Neurosci 34:5965–5970. CrossRef Medline

McMurray R, Islamov R, Murashov AK (2003) Raloxifene analog LY117018 enhances the regeneration of sciatic nerve in ovariectomized female mice. Brain Res 980:140–145. CrossRef Medline

McPhail LT, Fernandes KJ, Chan CC, Vanderluit JL, Tetzlaff W (2004) Axonal reinjury reveals the survival and re-expression of regeneration-associated genes in chronically axotomized adult mouse motoneurons. Exp Neurol 188:331–340. CrossRef Medline

Miller FD, Tetzlaff W, Bisby MA, Fawcett JW, Milner RJ (1989) Rapid induction of the major embryonic alpha-tubulin mRNA, T alpha 1, during nerve regeneration in adult rats. J Neurosci 9:1452–1463. Medline

Moore DL, Blackmore MG, Hu Y, Kaestner KH, Bixby JL, Lemmon VP, Goldberg JL (2009) KLF family members regulate intrinsic axon regeneration ability. Science 326:298–301. CrossRef Medline

Park KK, Liu K, Hu Y, Smith PD, Wang C, Cai B, Xu B, Connolly L, Kramvis I, Sahin M, He Z (2008) Promoting axon regeneration in the adult CNS by modulation of the PTEN/mTOR pathway. Science 322:963–966. CrossRef Medline

Popovich PG, Guan Z, Wei P, Huitinga I, van Rooijen N, Stokes BT (1999) Depletion of hematogenous macrophages promotes partial hindlimb recovery and neuroanatomical repair after experimental spinal cord injury. Exp Neurol 158:351–365. CrossRef Medline

Qin S, Zou Y, Zhang CL (2013) Cross-talk between KLF4 and STAT3 regulates axon regeneration. Nat Commun 4:2633. CrossRef Medline

Richardson PM, Issa VM, Aguayo AJ (1984) Regeneration of long spinal axons in the rat. J Neurocytol 13:165–182. CrossRef Medline

Schreyer DJ, Skene JH (1993) Injury-associated induction of GAP-43 expression displays axon branch specificity in rat dorsal root ganglion neurons. J Neurobiol 24:959–970. CrossRef Medline

Shen Y, Tenney AP, Busch SA, Horn KP, Cuascut FX, Liu K, He Z, Silver J, Flanagan JG (2009) PTPsigma is a receptor for chondroitin sulfate proteoglycan, an inhibitor of neural regeneration. Science 326:592–596. CrossRef Medline

Siebert JR, Middelton FA, Stelzner DJ (2010) Intrinsic response of thoracic propriospinal neurons to axotomy. BMC Neurosci 11:69. CrossRef Medline

So KF, Aguayo AJ (1985) Lengthy regrowth of cut axons from ganglion cells after peripheral nerve transplantation into the retina of adult rats. Brain Res 328:349–354. CrossRef Medline

Soderblom C, Luo X, Blumenthal E, Bray E, Lyapichev K, Ramos J, Krishnan V, Lai-Hsu C, Park KK, Tsoulfas P, Lee JK (2013) Perivascular fibroblasts form the fibrotic scar after contusive spinal cord injury. J Neurosci 33:13882–13887. CrossRef Medline

Starkey ML, Bartus K, Barritt AW, Bradbury EJ (2012) Chondroitinase ABC promotes compensatory sprouting of the intact corticospinal tract and recovery of forelimb function following unilateral pyramidotomy in adult mice. Eur J Neurosci 36:3665–3678. CrossRef Medline

Sun F, Park KK, Belin S, Wang D, Lu T, Chen G, Zhang K, Yeung C, Feng G, Yankner BA, He Z (2011) Sustained axon regeneration induced by co-deletion of PTEN and SOCS3. Nature 480:372–375. CrossRef Medline

Tetzlaff W, Alexander SW, Miller FD, Bisby MA (1991) Response of facial and rubrospinal neurons to axotomy: changes in mRNA expression for cytoskeletal proteins and GAP-43. J Neurosci 11:2528–2544. Medline

Tobias CA, Shumsky JS, Shibata M, Tuszynski MH, Fischer I, Tessler A, Murray M (2003) Delayed grafting of BDNF and NT-3 producing fibroblasts into the injured spinal cord stimulates sprouting, partially rescues axotomized red nucleus neurons from loss and atrophy, and provides limited regeneration. Exp Neurol 184:97–113. CrossRef Medline

Tom VJ, Houlé JD (2008) Intraspinal microinjection of chondroitinase ABC following injury promotes axonal regeneration out of a peripheral nerve graft bridge. Exp Neurol 211:315–319. CrossRef Medline

Tom VJ, Kadakia R, Santi L, Houlé JD (2009a) Administration of chondroitinase ABC rostral or caudal to a spinal cord injury site promotes anatomical but not functional plasticity. J Neurotrauma 26:2323–2333. CrossRef Medline

Tom VJ, Sandrow-Feinberg HR, Miller K, Santi L, Connors T, Lemay MA, Houlé JD (2009b) Combining peripheral nerve grafts and chondroitinase promotes functional axonal regeneration in the chronically injured spinal cord. J Neurosci 29:14881–14890. CrossRef Medline

Tom VJ, Sandrow-Feinberg HR, Miller K, Domitrovich C, Bouyer J, Zhukareva V, Klaw MC, Lemay MA, Houlé JD (2013) Exogenous BDNF enhances the integration of chronically injured axons that regenerate through a peripheral nerve grafted into a chondroitinase-treated spinal cord injury site. Exp Neurol 239:91–100. CrossRef Medline

Wang Z, Reynolds A, Kirry A, Nienhaus C, Blackmore MG (2015) Overexpression of sox11 promotes corticospinal tract regeneration after spinal injury while interfering with functional recovery. J Neurosci 35:3139–3145. CrossRef Medline

Wanner IB, Anderson MA, Song B, Levine J, Fernandez A, Gray-Thompson Z, Ao Y, Sofroniew MV (2013) Glial scar borders are formed by newly proliferated, elongated astrocytes that interact to corral inflammatory and fibrotic cells via STAT3-dependent mechanisms after spinal cord injury. J Neurosci 33:12870–12886. CrossRef Medline

Wu D, Raafat A, Pak E, Clemens S, Murashov AK (2012) Dicer-microRNA pathway is critical for peripheral nerve regeneration and functional recovery *in vivo* and regenerative axonogenesis in vitro. Exp Neurol 233:555–565. CrossRef Medline

Yan L, Findlay GM, Jones R, Procter J, Cao Y, Lamb RF (2006) Hyperactivation of mammalian target of rapamycin (mTOR) signaling by a gain-of-function mutant of the Rheb GTPase. J Biol Chem 281:19793–19797. CrossRef Medline

Ye JH, Houle JD (1997) Treatment of the chronically injured spinal cord with neurotrophic factors can promote axonal regeneration from supraspinal neurons. Exp Neurol 143:70–81. CrossRef Medline

Zhou S, Shen D, Wang Y, Gong L, Tang X, Yu B, Gu X, Ding F (2012) microRNA-222 targeting PTEN promotes neurite outgrowth from adult dorsal root ganglion neurons following sciatic nerve transection. PLoS One 7:e44768. CrossRef Medline

Zukor K, Belin S, Wang C, Keelan N, Wang X, He Z (2013) Short hairpin RNA against PTEN enhances regenerative growth of corticospinal tract axons after spinal cord injury. J Neurosci 33:15350–15361. CrossRef Medline

Zuo J, Ferguson TA, Hernandez YJ, Stetler-Stevenson WG, Muir D (1998) Neuronal matrix metalloproteinase-2 degrades and inactivates a neurite-inhibiting chondroitin sulfate proteoglycan. J Neurosci 18:5203–5211. Medline